Figure S1

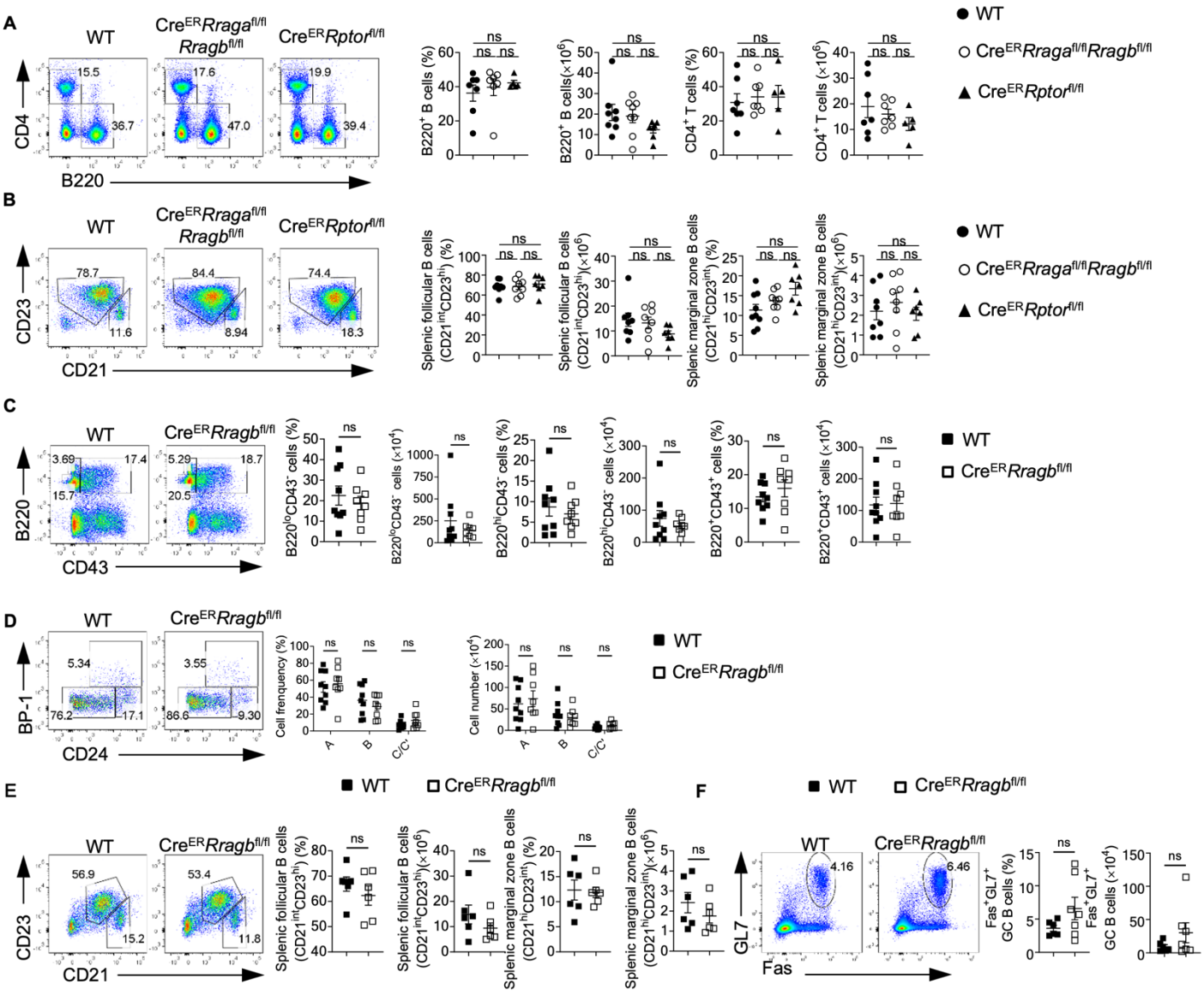

Figure S1. RagB deficiency doesn't affect early B cell development in BM and peripheral B cells. (A) Representative flow plots of splenic CD4$^+$ T cells and B220$^+$ B cells from WT mice (n = 7), *Cre^{ER}Rraga$^{fl/fl}$Rragb$^{fl/fl}$* (n = 7), and *Cre^{ER}Rptor$^{fl/fl}$* (n = 5). Right, summaries of the percentages and numbers of splenic CD4$^+$ T cells (gated on TCR-b$^+$ cells) and B220$^+$ B cells. (B) flow plots of splenic follicular B cells (CD21^{int}CD23^{hi}) or marginal zone (CD21^{hi}CD23^{int}) from WT mice (n = 8), *Cre^{ER}Rraga$^{fl/fl}$Rragb$^{fl/fl}$* (n = 8), and *Cre^{ER}Rptor$^{fl/fl}$* (n = 7). Right, summaries of the percentages and numbers of splenic follicular B cells (CD21^{int}CD23^{hi}) or marginal zone (CD21^{hi}CD23^{int}). (C) Representative flow plots of bone marrow B220 and CD43 expression from WT (n = 9), and Cre^{ER}*Rragb$^{fl/fl}$* (n = 8) mice. Right, summaries of the percentages and numbers of B220^{lo}CD43$^-$, B220^{hi}CD43$^-$ and B220$^+$CD43$^+$ cells. (D) Representative flow plots of BP-1 and CD24 expression in BM B220$^+$CD43$^+$IgM$^-$ B cell precursors from WT (n = 9) and Cre^{ER}*Rragb$^{fl/fl}$* (n = 8) mice.

Right, summary of the percentages and numbers of fraction A ($CD24^{-}BP\text{-}1^{-}$), fraction B ($CD24^{+}BP\text{-}1^{-}$), and fraction C/C′($CD24^{+}BP\text{-}1^{+}$) cells. (E) Representative flow plots of splenic follicular B cells ($CD21^{int}CD23^{hi}$) or marginal zone ($CD21^{hi}CD23^{int}$) from WT (n = 9) and Cre^{ER}*Rragb*$^{fl/fl}$ (n = 8) mice. Right, summaries of the percentages and cell numbers of splenic follicular B cells ($CD21^{int}CD23^{hi}$) or marginal zone ($CD21^{hi}CD23^{int}$) B cells. (F) Representative flow plots of GL-7 and Fas expression in lymphocytes from the Peyer's patches from WT (n = 6) and Cre^{ER}*Rragb*$^{fl/fl}$ (n = 7) mice. Right, summary of the percentages and numbers of GC ($GL\text{-}7^{+}Fas^{+}$) B cells. Data in graphs represent mean ± SEM. ns, not significant. One-way ANOVA (A and B), two-way ANOVA (D), two-tailed Student’s t test (C, E and F).

Figure S2

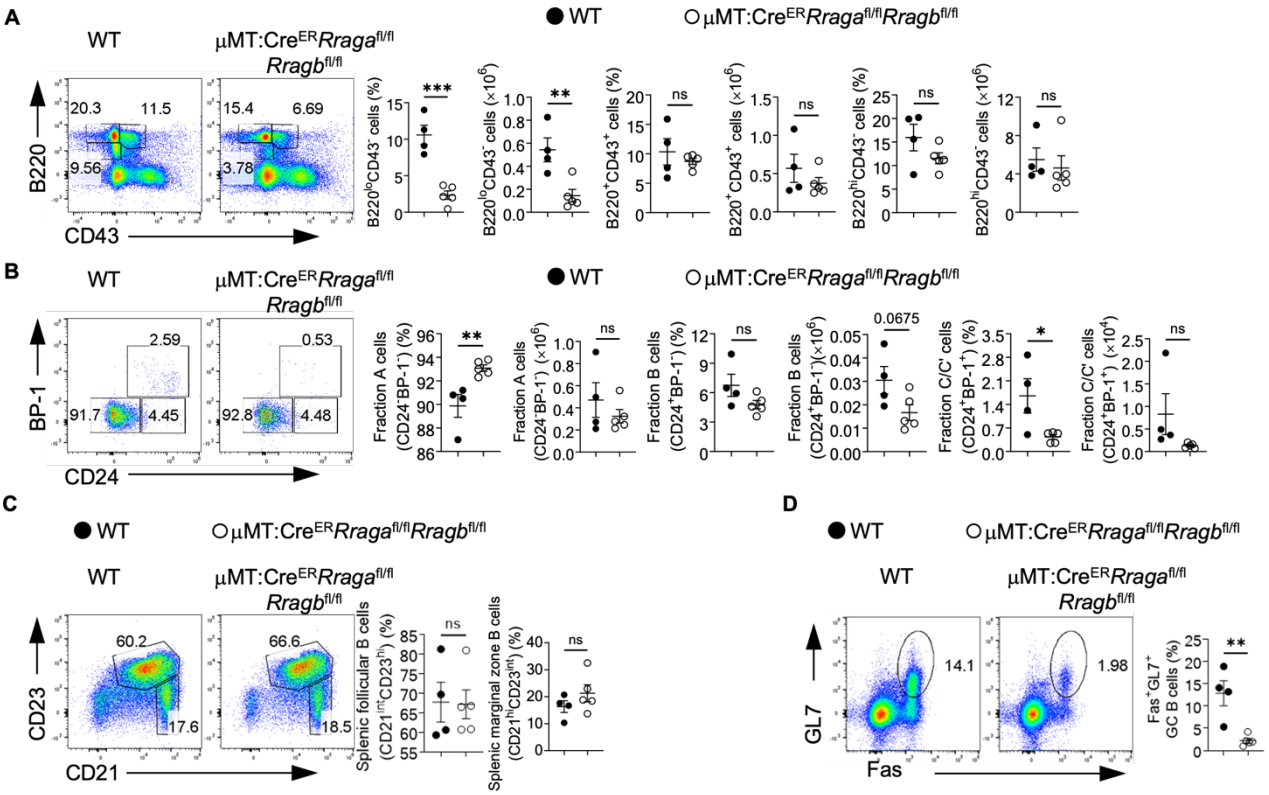

Figure S2. Rag-GTPases deficiency intrinsically disrupts B cell development. (A-D) Tamoxifen was administered to μMT:Cre^{ER}*Rraga*$^{fl/fl}$*Ragb*$^{fl/fl}$ (n = 5), and WT (n = 4) chimera mice by oral gavage daily for 4 consecutive days. Mice were analyzed 7 days after the last injection. (A) Representative flow plots of bone marrow B220 and CD43 expression from μMT:Cre^{ER}*Rraga*$^{fl/fl}$*Ragb*$^{fl/fl}$, and WT chimera mice. Right, summaries of the percentages and numbers of B220^{lo}CD43^{-}, B220^{hi}CD43^{-} and B220^{+}CD43^{+} cells. (B) Representative flow plots of BP-1 and CD24 expression in BM B220^{+}CD43^{+}IgM^{-} B cell precursors from μMT:Cre^{ER}*Rraga*$^{fl/fl}$*Ragb*$^{fl/fl}$, and WT chimera mice. Right, summaries of the percentages and numbers of bone marrow fraction A (CD24^{-}BP-1^{-}), fraction B (CD24^{+}BP-1^{-}), and fraction C/C′(CD24^{+}BP-1^{+}) cells. (C) Representative flow plots of splenic follicular B cells (CD21^{int}CD23^{hi}) or marginal zone (CD21^{hi}CD23^{int}) from μMT:Cre^{ER}*Rraga*$^{fl/fl}$*Ragb*$^{fl/fl}$, and WT chimera mice. Right, summaries of the percentages of splenic follicular B cells (CD21^{int}CD23^{hi}) or marginal zone (CD21^{hi}CD23^{int}) B cells. (D) Representing flow plots of Fas and GL-7 expression on B cells from the Peyer's patches of μMT:Cre^{ER}*Rraga*$^{fl/fl}$*Ragb*$^{fl/fl}$, and WT chimera mice. Right, summary of the percentages of GC (GL-7^{+}Fas^{+}) B cells. Data in graphs represent mean ± SEM. ns, not significant. *p < 0.05, **p < 0.01, ***p < 0.001, two-tailed Student's t test was used.

Figure S3

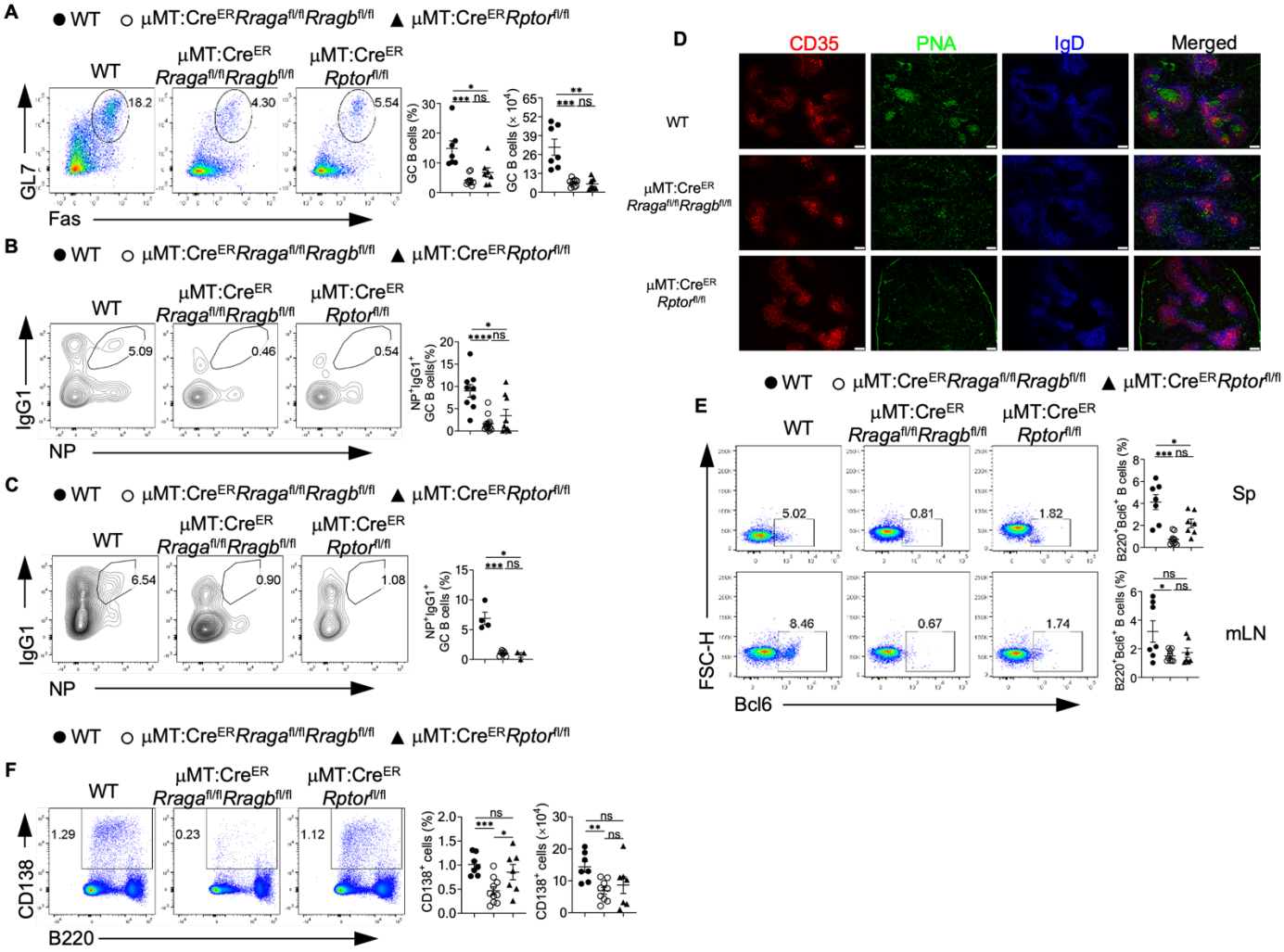

Figure S3. Rag-GTPases deficiency reduces GC formation and antibody production independent of mTORC1 in peptide immunization. (A-F) Tamoxifen was administered to μMT:Cre^{ER}*Rraga*$^{fl/fl}$*Ragb*$^{fl/fl}$, μMT:Cre^{ER}*Rptor*$^{fl/fl}$, and WT chimera mice by oral gavage daily for 4 consecutive days. Mice were immunized intraperitoneally (100 mg NP-OVA/alum) 7 days after the last injection. (A) Representative flow plots of GL-7 and Fas expression on B cells from the mesenteric lymph node (mLN) of immunized WT (n = 7), μMT:Cre^{ER}*Rraga*$^{fl/fl}$*Ragb*$^{fl/fl}$ (n = 9), and μMT:Cre^{ER}*Rptor*$^{fl/fl}$ (n = 7) chimera mice. Right, summary of the percentages and numbers of GC (GL-7^{+}Fas^{+}) B cells. (B) Representative flow plots of NP^{+}IgG1^{+} GC B cells from the spleen of immunized WT (n = 9), μMT:Cre^{ER}*Rraga*$^{fl/fl}$*Ragb*$^{fl/fl}$ (n = 13), and μMT:Cre^{ER}*Rptor*$^{fl/fl}$ (n = 9) chimera mice. Right, summary of the percentages of NP^{+}IgG1^{+} GC B cells. (C) Representative flow plots of NP^{+}IgG1^{+} GC B cells from the mLN of immunized WT (n = 4), μMT:Cre^{ER}*Rraga*$^{fl/fl}$*Ragb*$^{fl/fl}$ (n = 7), and μMT:Cre^{ER}*Rptor*$^{fl/fl}$ (n = 3) chimera mice. Right, summary of the percentages of NP^{+}IgG1^{+} GC B cells. (D)

Cryosections from the spleens of immunized WT, μMT:Cre^{ER}*Rraga*$^{fl/fl}$*Rragb*$^{fl/fl}$, and μMT:Cre^{ER}*Rptor*$^{fl/fl}$ chimera mice were stained for GC B cells (anti-PNA). Scale bar, 50 mm. Anti-IgD stains for FoBs, anti-CD35 stains for follicular dendritic cells (LZ). (E) Representative flow plots of Bcl6 expression on total B cells from both spleen (upper panel) and mLN (lower panel) of immunized WT (n = 7), μMT:Cre^{ER}*Rraga*$^{fl/fl}$*Rragb*$^{fl/fl}$ (n = 9), and μMT:Cre^{ER}*Rptor*$^{fl/fl}$ (n = 7) chimera mice. Right, summary of the percentage of Bcl6^{+} B cells on B cells. (F) Representative flow plots of CD138 and B220 expression in mLN of WT (n = 7), μMT:Cre^{ER}*Rraga*$^{fl/fl}$*Rragb*$^{fl/fl}$ (n = 9), and μMT:Cre^{ER}*Rptor*$^{fl/fl}$ (n = 7) mice. Right, summary of the percentages and numbers of CD138^{+} cells. Data in graphs represent mean ± SEM. ns, not significant. *p < 0.05, **p < 0.01, ***p < 0.001, and ****p < 0.0001, one-way ANOVA was used.

Figure S4

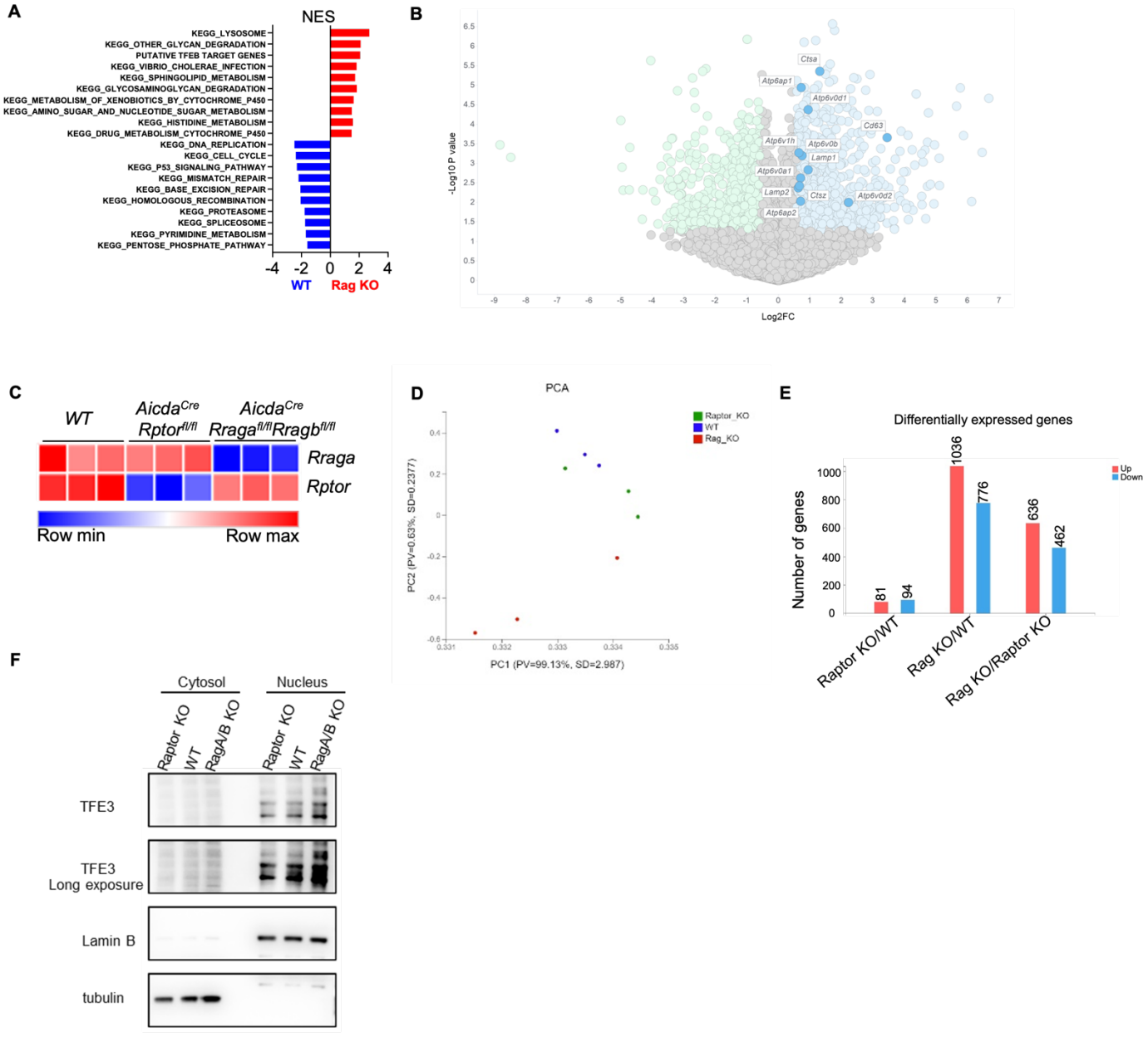

Figure S4. Rag-GTPases regulate TFEB/TFE3 axis in B cells. (A) Bulk RNA sequencing was performed on the B cells activated with LPS/IL-4/BAFF for 72 h, then GSEA was conducted on differentially expressed genes (DEGs), and significantly enriched pathways were plotted according to NES (normalized enrichment score). (B) Volcano plot of the lysosome genes enriched in RagA/RagB deficient B cells. (C-E) GC B cells were sorted from immunized *Aicda*^{Cre}*Rraga*$^{fl/fl}$*Rragb*$^{fl/fl}$, *Aicda*^{Cre}*Rptor*$^{fl/fl}$, and WT mice, and conducted bulk RNA sequencing. (C) *Rraga,* and *Rptor* levels from the bulk RNA sequencing data. (D) PCA plot from the bulk RNA sequencing analysis. (E) Statistics of differently expressed genes from different comparisons. (F) Cytosolic and nuclear

proteins were isolated from the B cells activated with LPS/IL-4/BAFF for 72 h. Expression of TFE3 was examined by immunoblot. Lamin B was used as a nuclear control, tubulin was used as a cytosol control.

Figure S5

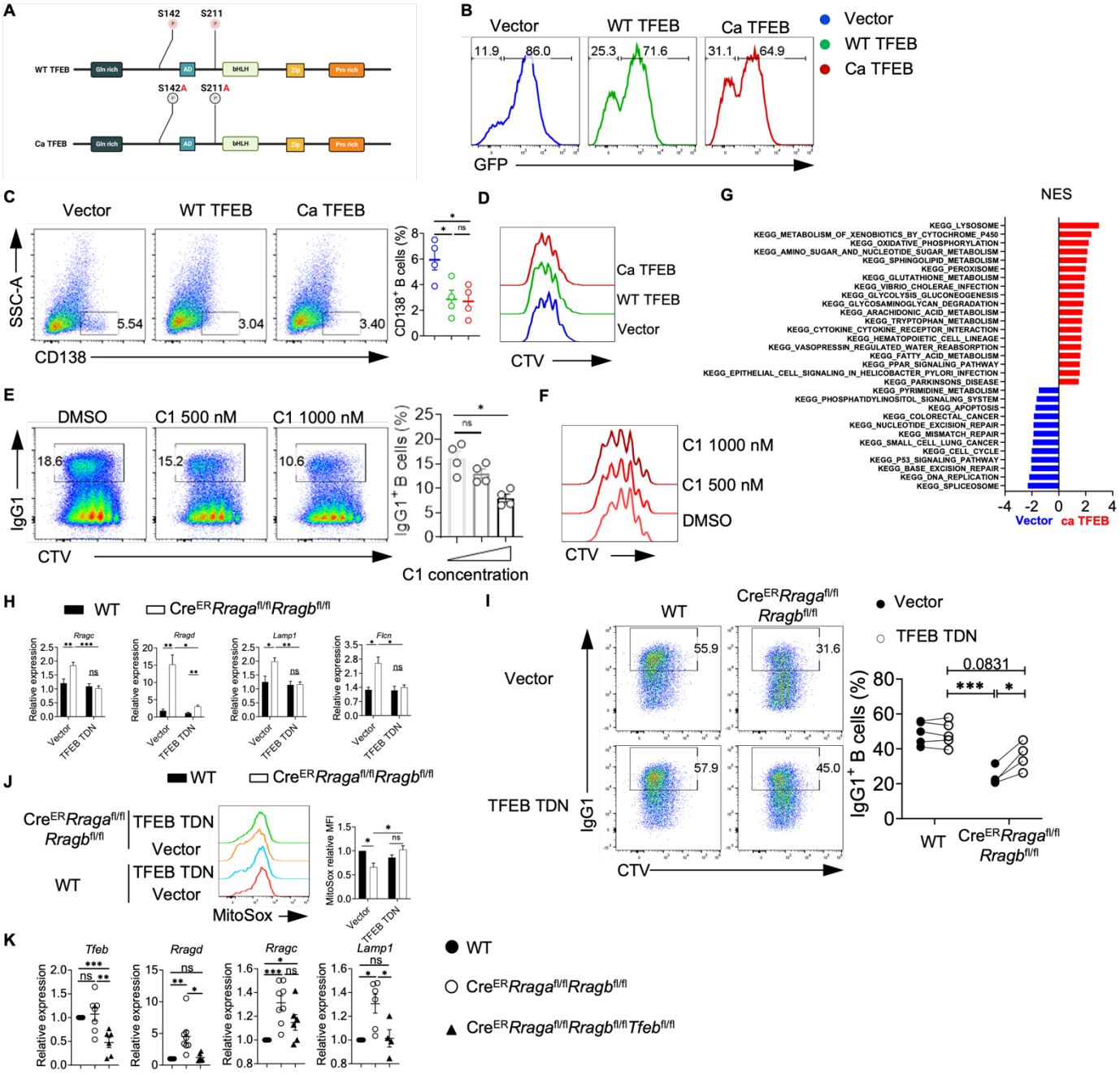

Figure S5. TFEB plays a critical role in Rag GTPases regulated B cell function. (A) Schematic of the experimental design for making WT TFEB and Ca TFEB plasmids. (B) Representative histogram of GFP expression on the vector, WT TFEB or Ca TFEB transduced B cells. (C) Representative flow plots of $CD138^+$ expression on vector, WT TFEB, and Ca TFEB transduced GFP^+ B cells. (D) Representative flow plots of CTV dilution from vector, WT TFEB, and Ca TFEB transduced GFP^+ B cells. (E) Representative flow plots of IgG1 and CTV expression activated in LPS/IL-4/BAFF with different concentrations of compound C1 for 72 h. Right,

summary of IgG1$^+$ B cells. (F) Representative flow plots of CTV dilution from different concentrations of compound C1 treated B cells. (G) GFP$^+$ B cells were sorted from vector, or Ca TFEB transduced B cells, and bulk RNA sequencing was conducted on these samples. GSEA was performed on the DEGs, and significantly enriched pathways were plotted according to NES. (H) Splenic B cells from Cre^{ER}*Rraga*$^{fl/fl}$*Rragb*$^{fl/fl}$ (n = 5), and WT (n = 5) mice were transduced with vector or TFEB TDN, then B cells were cultured with LPS/IL-4/BAFF for 72 h, TFEB downstream target genes were examined. (I) Spenic B cells from Cre^{ER}*Rraga*$^{fl/fl}$*Rragb*$^{fl/fl}$ (n = 4), and WT (n = 5) mice were transduced with vector or TFEB TDN, and IgG1$^+$ B cells were measured. Right, summary of the IgG1$^+$ B cells. (J) Spenic B cells from Cre^{ER}*Rraga*$^{fl/fl}$*Rragb*$^{fl/fl}$ and WT mice were transduced with vector or TFEB TDN, MitoSox was measured after activation with LPS/IL-4/BAFF for 72 h. Right, summary of MitoSox level (Relative to vector transduced WT B cells). (K) TFEB downstream target genes were measured on the activated B cells from WT (n = 4-6), Cre^{ER}*Rraga*$^{fl/fl}$*Rragb*$^{fl/fl}$ (n = 6-8), and Cre^{ER}*Rraga*$^{fl/fl}$*Rragb*$^{fl/fl}$*Tfeb*$^{fl/fl}$ (n = 4-6) mice. Data in graphs represent mean ± SEM. ns, not significant. *p < 0.05, **p < 0.01, and ***p < 0.001, one-way ANOVA (C, E and K), two-way ANOVA (H, I and J).

Figure S6

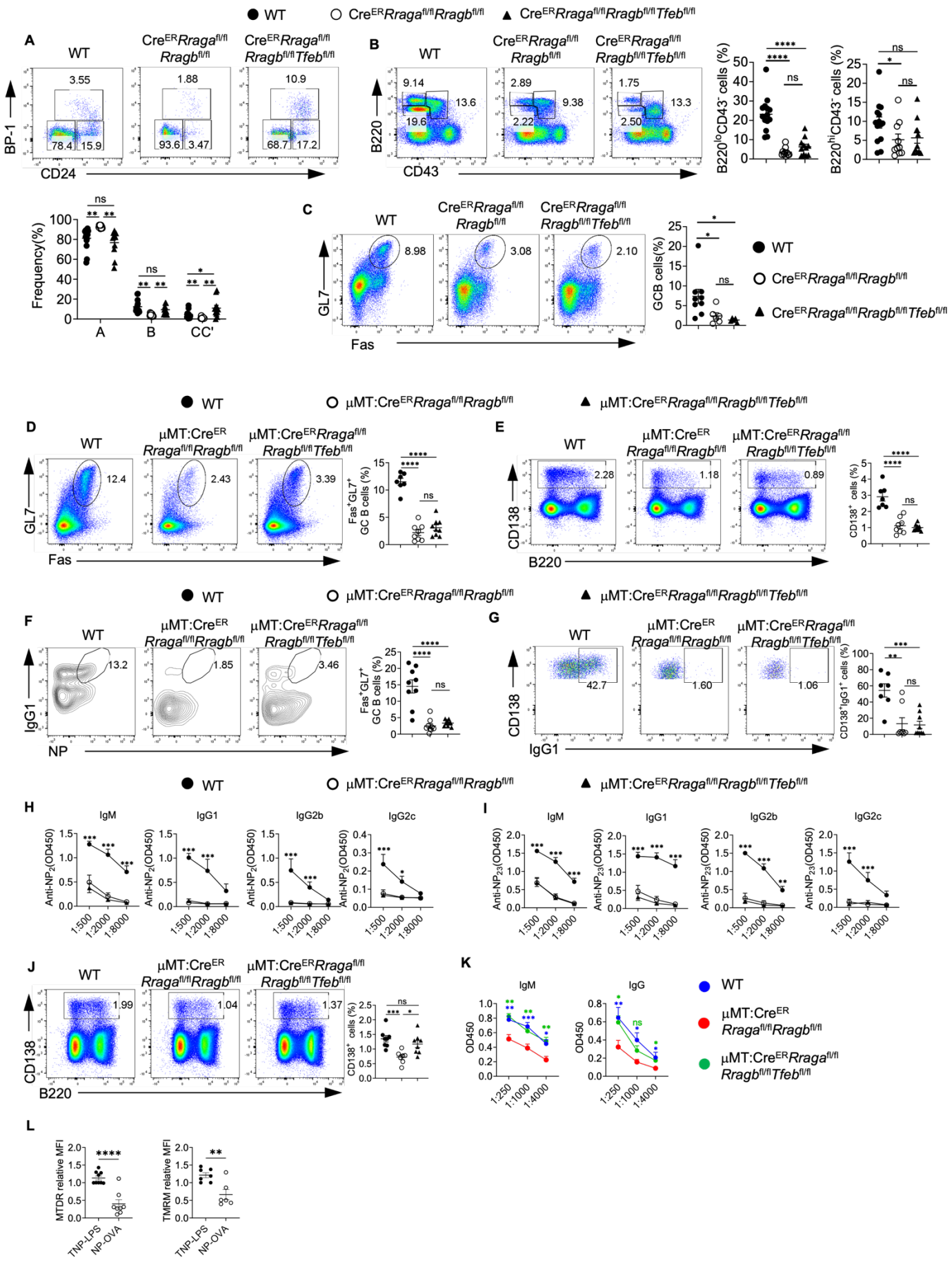

Figure S6. Abrogating TFEB rescues the deficiency in Rag-GTPases KO mice in context-dependent manner. (A-C)Tamoxifen was administered to animals intraperitoneally daily for 4 consecutive days. Mice were sacrificed and analyzed 7 days after the last injection. (A) Representative flow plots of BP-1 and CD24 expression in BM $B220^{+}CD43^{+}IgM^{-}$ B cell precursors from WT (n = 14), Cre^{ER}*Rraga*$^{fl/fl}$*Rragb*$^{fl/fl}$ (n = 10), and Cre^{ER}Rraga$^{fl/fl}$*Rragb*$^{fl/fl}$*Tfeb*$^{fl/fl}$ (n = 11) mice. Right, summary of the percentages of fraction A ($CD24^{-}BP\text{-}1^{-}$), fraction B ($CD24^{+}BP\text{-}1^{-}$), and fraction C/C′ ($CD24^{+}BP\text{-}1^{+}$) cells. (B) Representative flow plots of B220 and CD43 expression in BM lymphocytes from Cre^{ER}*Rraga*$^{fl/fl}$*Rragb*$^{fl/fl}$ (n = 10), Cre^{ER}Rraga$^{fl/fl}$*Rragb*$^{fl/fl}$*Tfeb*$^{fl/fl}$ (n = 11), and WT (n = 14) mice. Right, summaries of the percentages of $B220^{lo}CD43^{-}$ and $B220^{hi}CD43^{-}$ cells. (C) Representative flow plots of GL-7 and Fas expression in lymphocytes from the Peyer's patches of WT (n = 9), Cre^{ER}*Rraga*$^{fl/fl}$*Rragb*$^{fl/fl}$ (n = 6), and Cre^{ER}Rraga$^{fl/fl}$*Rragb*$^{fl/fl}$*Tfeb*$^{fl/fl}$ (n = 5) mice. Right, summary of the percentages of GC ($GL\text{-}7^{+}Fas^{+}$) B cells. (D-I) Tamoxifen was administered to animals by oral gavage daily for 4 consecutive days. Mice were immunized intraperitoneally (100 mg NP-OVA/alum) 7 days after the last injection. (D) Representative flow plots of GL-7 and Fas expression on splenic B cells from the spleen of WT (n = 7), μMT:Cre^{ER}*Rraga*$^{fl/fl}$*Rragb*$^{fl/fl}$ (n = 8), and μMT:Cre^{ER}*Rraga*$^{fl/fl}$*Rragb*$^{fl/fl}$*Tfeb*$^{fl/fl}$ (n = 9) immunized chimera mice. Right, summary of the percentages of GC ($GL\text{-}7^{+}Fas^{+}$) B cells. (E) Representative flow plots of CD138 and B220 expression in spleens from immunized WT (n = 7), μMT:Cre^{ER}*Rraga*$^{fl/fl}$*Rragb*$^{fl/fl}$ (n = 8), and μMT:Cre^{ER}*Rraga*$^{fl/fl}$*Rragb*$^{fl/fl}$*Tfeb*$^{fl/fl}$ (n = 9) chimera mice. Right, summary of the percentages of $CD138^{+}$ cells. (F) Representative flow plots of $NP^{+}IgG1^{+}$ GC B cells from the spleen of immunized WT (n = 7), μMT:Cre^{ER}*Rraga*$^{fl/fl}$*Rragb*$^{fl/fl}$ (n = 9), and μMT:Cre^{ER}*Rraga*$^{fl/fl}$*Rragb*$^{fl/fl}$*Tfeb*$^{fl/fl}$ (n = 9) chimera mice. (G) Representative flow plots of splenic $CD138^{+}IgG1^{+}$ cells from immunized WT (n = 7), μMT:Cre^{ER}*Rraga*$^{fl/fl}$*Rragb*$^{fl/fl}$ (n = 8), and μMT:Cre^{ER}*Rraga*$^{fl/fl}$*Rragb*$^{fl/fl}$*Tfeb*$^{fl/fl}$ (n = 9) chimera mice. (H) high-affinity NP-specific antibodies of all classes were measured using the sera of immunized WT (n = 6), μMT:Cre^{ER}*Rraga*$^{fl/fl}$*Rragb*$^{fl/fl}$ (n = 8), and μMT:Cre^{ER}*Rraga*$^{fl/fl}$*Rragb*$^{fl/fl}$*Tfeb*$^{fl/fl}$ (n = 9) chimera mice. (I) Total NP-specific antibodies of all classes were measured using the sera of immunized WT (n = 6), μMT:Cre^{ER}*Rraga*$^{fl/fl}$*Rragb*$^{fl/fl}$ (n = 8), and μMT:Cre^{ER}*Rraga*$^{fl/fl}$*Rragb*$^{fl/fl}$*Tfeb*$^{fl/fl}$ (n = 9) chimera mice. (J) Representative flow plots of splenic $CD138^{+}$ cells from TNP-LPS immunized WT (n = 8), μMT:Cre^{ER}*Rraga*$^{fl/fl}$*Rragb*$^{fl/fl}$ (n = 7), and μMT:Cre^{ER}*Rraga*$^{fl/fl}$*Rragb*$^{fl/fl}$*Tfeb*$^{fl/fl}$ (n = 8) chimera mice. (K) anti-TNP antibody titers in the sera of immunized WT (n = 8), μMT:Cre^{ER}*Rraga*$^{fl/fl}$*Rragb*$^{fl/fl}$ (n = 7), and μMT:Cre^{ER}*Rraga*$^{fl/fl}$*Rragb*$^{fl/fl}$*Tfeb*$^{fl/fl}$ (n = 8) chimera mice. (L)

WT mice were immunized with TNP-LPS or NP-OVA/alum, TMRM or MTDR on $CD138^+$ cells were measured at day 9 (NP-OVA/alum) or 7 (TNP-LPS) post-immunization. Data in graphs represent mean ± SEM. ns, not significant. *$p < 0.05$, **$p < 0.01$, ***$p < 0.001$, and ****$p < 0.0001$, one-way ANOVA (B, C, D, E, F, G and J), two-way ANOVA (A, H, I and K), two-tailed Student's t test (L).